Supplementary Information

Deciphering the dual function of silicon dioxide protective layer in regulating lithium ion deposition

Tianlai Wu,[ab] Weicai Zhang,[ab] Jiawen Cai,[a] Mingtao Zheng,[ab] Hang Hu,[ab] Xiaoyuan Yu,[ab] Dan Shao, *[c] Yong Xiao,[ab] Yingliang Liu,*[ab] Yeru Liang*[ab]

[a] *Key Laboratory for Biobased Materials and Energy of Ministry of Education, Guangdong Provincial Engineering Technology Research Center for Optical Agriculture, College of Materials and Energy, South China Agricultural University, Guangzhou, 510642, China*

[b] *Guangdong Laboratory of Lingnan Modern Agriculture, Guangzhou, 510642, China*

[c] *Guangdong Key Laboratory of Battery Safety, Guangzhou Institute of Energy Testing, Guangzhou, 511447, China*

*Corresponding author.
E-mail address: shaod1005@163.com (D. Shao); tliuyl@scau.edu.cn (Y.L. Liu); liangyr@scau.edu.cn (Y.R. Liang)

Experimental section

Materials

Li metal foils (600 um thickness, 16 mm diameter) were purchased from China Energy Lithium Co., Ltd. Tetraethoxysilane was purchased from Ltd. Fortune (Tianjin) Chemical Reagent Co., Ltd. Celgard 2500 polypropylene membranes was purchased from Guangdong Canrd New Energy Technology Co., Ltd. $LiNi_{0.5}Co_{0.2}Mn_{0.3}O_2$ was purchased from Shenzhen Kejing Zhida Technology Co., Ltd. Ethylacetate, Lithium hexafluorophosphate ($LiPF_6$), Diethyl carbonate (DEC) and Ethylene carbonate (EC) were purchased from Aladdin Chemical Co., Ltd.

Synthesis of protected Li

The preparation of the protected Li can be described as follow. Firstly, 20 uL TEOS was dropped evenly onto the surface of Li metal in the glove box. After standing for 10 min, the excess TEOS on the surface of Li metal was slowly sucked away with a pipette. Finally, the Li metal was dried in glove box at room temperature for 12 hours.

Materials characterization

Scanning electron microscopy (SEM, HITACHISU8220) and energy dispersive spectroscopy (EDS, X-Max) were employed to characterize the morphology and elemental distribution, respectively. X-ray diffraction (XRD, Ultima IV) and Fourier-transforms infrared (FTIR, Vertex 70) were carried out to characterize the substance structure and substance composition, respectively.

Electrochemical measurements

The electrochemical performances of pristine Li, protected Li were evaluated using two-electrode battery configuration. Electrochemical experiments were performed by using CR2032-type coin batteries. All electrochemical performances were measured at room temperature.

Li||Li symmetric cell assembly and electrochemical measurements

Symmetric cells were assembled using pristine Li, protected Li as the working electrode and the anode, respectively. The Celgard 2500 membranes and 1.0 M $LiPF_6$ in EC/DEC (1:1 vol) were used as separator and electrolyte, respectively. The amount of electrolyte used was 60 μL.

The as-assembled symmetric batteries were monitored in galvanostatic mode using a Neware battery test system (BTS 7.6.x, Neware). The systematic cells were cycled at a current density of 0.5 mA cm^{-2} with a capacity of 0.5 mAh cm^{-2}, and also cycled at the current density of 1.0 mA cm^{-2} with a capacity of 1.0 mAh cm^{-2}. Moreover, the Li||Li systematic cells were cycled at the current density of 1, 3, 5 mA cm^{-2} with a capacity of 1.0 mAh cm^{-2}. EIS analyses were conducted using an electrochemical work station (CHI 660D Chen Hua) in the frequency range from 100 kHz to 100 mHz with a voltage amplitude of 5 mV. Cyclic voltammetry (CV) was performed on an electrochemical work station (CHI 660D Chen Hua) with a voltage amplitude of 5 mV. A fixed sweep rate of 1 mV s^{-1} was employed with the voltage range from -100 mV to 100 mV. The exchange current density was calculated using a linear fit of Tafel plots (from 100 mV to 50 mV). The determination of activation energies related to Li ion diffusion through SEI layer was based on the temperature-

dependent EIS measurement of Li||Li symmetric cell. The activation energy can be acquired according to the relation of E_a=-19.144xslope (kJ mol^{-1}), where the slope can be pre-obtained based on the linear fitting results. The nucleation overpotential was tested by directly plating Li on pristine Li and protected Li at various current densities.

To probe the effect of deposition amount of Li on the impedance, various amounts of Li was deposited on pristine Li and protected Li at 0.5 mA cm^{-2}, then the EIS of the batteries were tested by an electrochemical workstation. To probe the effect of cycling numbers on the impedance, the Li||Li symmetric cells were cycling at a current density of 1 mA cm^{-2} and 1 mAh cm^{-2} and the EIS of the batteries was tested by an electrochemical workstation after various cycles.

To evaluate the morphology of Li metal anodes after long-term Li plating/stripping, the Li||Li symmetric cells were assembled and cycling at a current density of 1 mA cm^{-1} with a capacity of 1 mAh cm^{-2} for 50 cycles.

Li ||NCM523 cell assembly and electrochemical measurements

Li||NCM523 cells were assembled using pristine Li and protected Li as the anode, respectively. The Celgard 2500 membranes and 1.0 M $LiPF_6$ in EC/DEC (1:1 vol) were used as separator and electrolyte, respectively. The amount of electrolyte used was 60 μL. The cathode of NCM523 was cut into circular disks with an area of 1.13 cm^2 and a total mass loading density was about 9 mg cm^{-2}. The Li||NCM523 cells were cycled within a voltage range of 3.0-4.3 V.

$$4LiOH+Si(OR)_4 \longrightarrow 4ROLi+SiO_2+2H_2O$$

Eq. S1. Chemical reaction between Li metal anode and TEOS.

$$5SiO_2+4Li^{+}+4e^{-} \longrightarrow 2Li_2Si_2O_5+Si$$

Eq. S2. Electrochemical reaction between Li^+ and SiO_2.

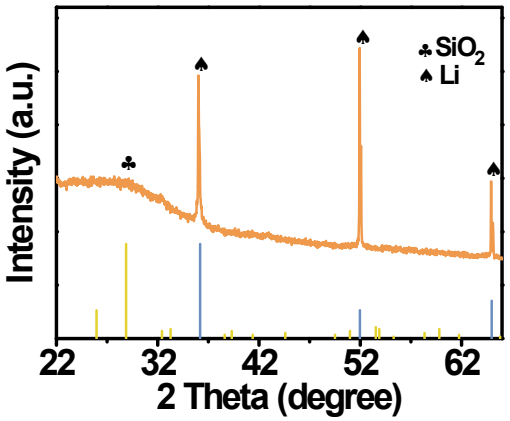

Fig.S1 XRD pattern of protected Li.

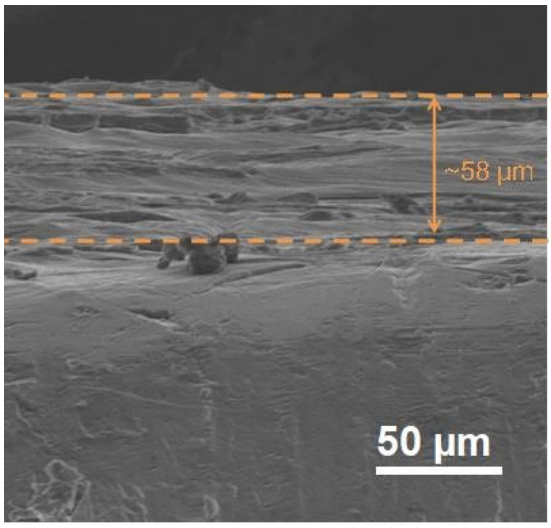

Fig. S2 Cross-sectional SEM image of protected Li.

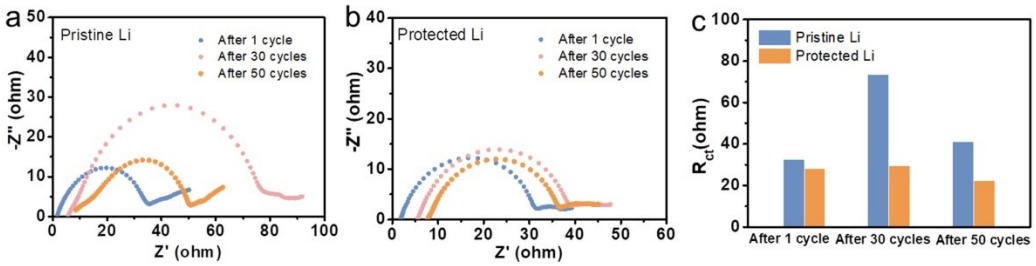

Fig. S3 Nyquist plots of (a) pristine Li and (b) protected Li after different cycling numbers. (c) Interfacial impendence of pristine Li and protected Li after different cycling numbers.

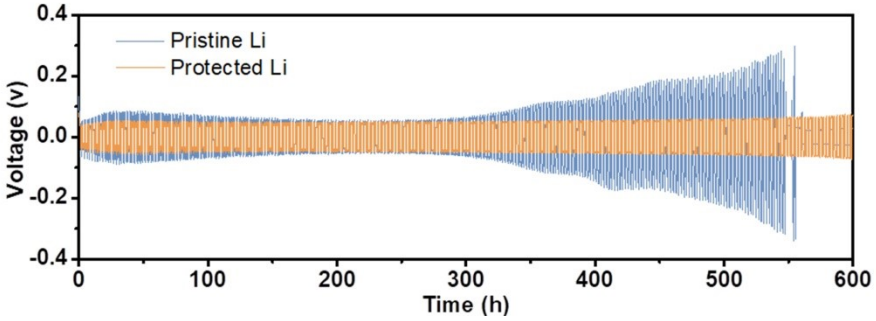

Fig. S4 Galvanostatic cycling performance of Li||Li symmetrical cell at 0.5 mA cm^{-2} and 0.5 mAh cm^{-2}.

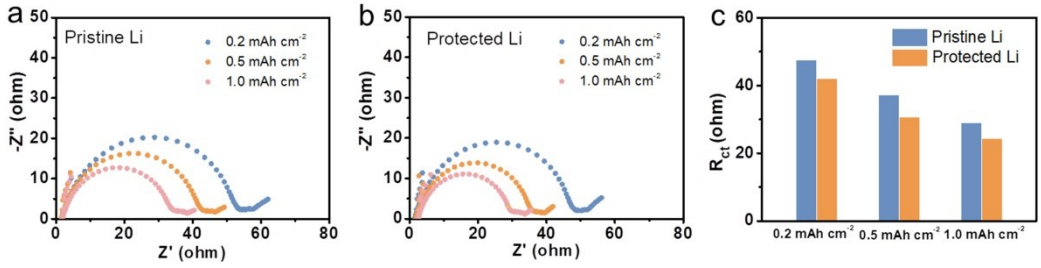

Fig. S5 Nyquist plots of (a) pristine Li and (b) protected Li with the increase of Li deposition. (c) Interfacial impendence of pristine Li and protected Li after deposing different capacity of Li.

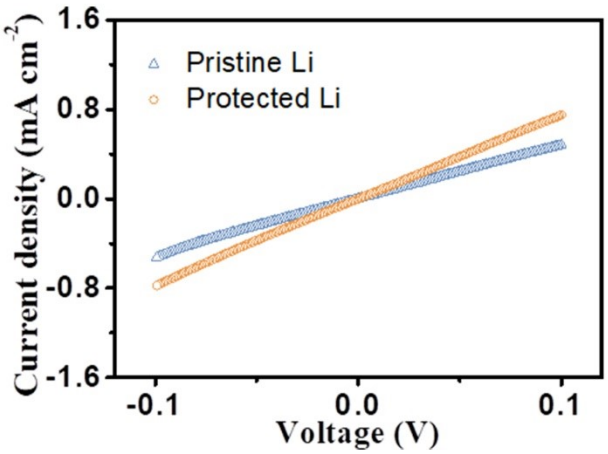

Fig. S6 CV measurement of Li||Li symmetric cells assembled with pristine Li and protected Li, respectively.

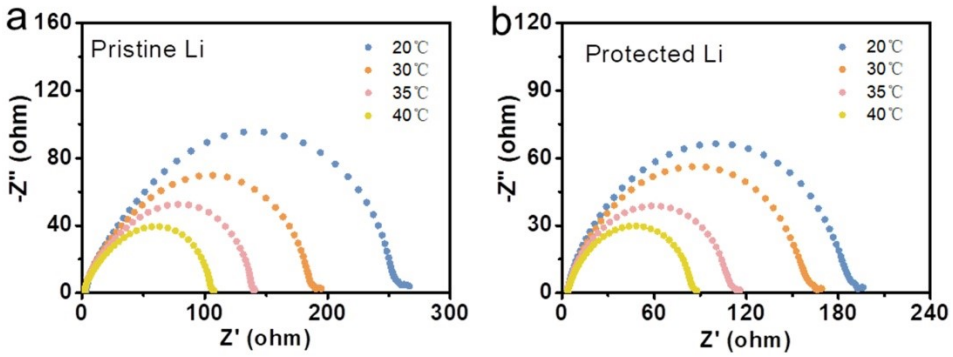

Fig. S7 Nyquist plots of (a) pristine Li and (b) protected Li at the different temperature.

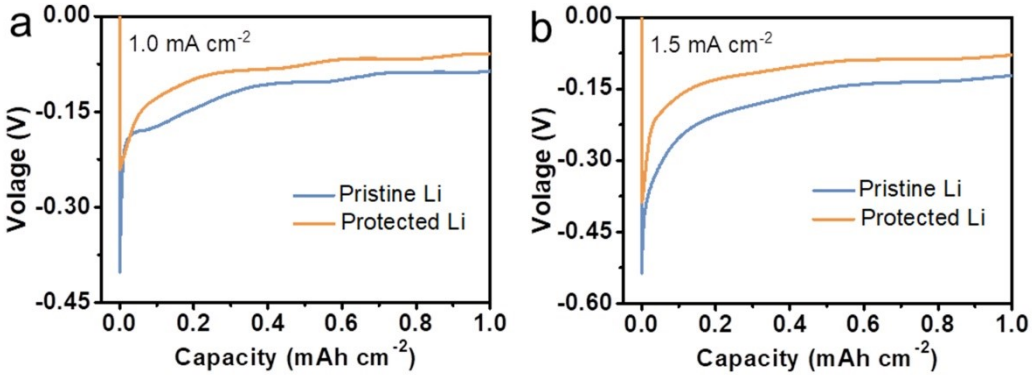

Fig. S8 Voltage-capacity curves of (a) pristine Li and (b) protected Li during Li nucleation at 1.0 and 1.5 mA cm^{-2}, respectively.

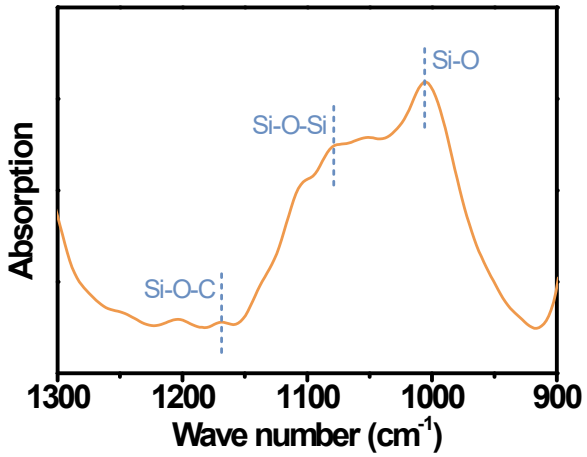

Fig. S9 FTIR spectra of protected Li after depositing Li with 0.5 mAh cm^{-2}.

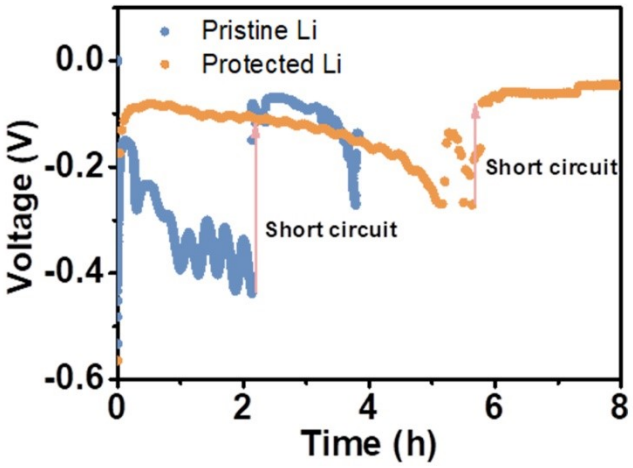

Fig. S10 Constant current polarization test of pristine Li and protected Li at a current density of 4 mA cm^{-2}.

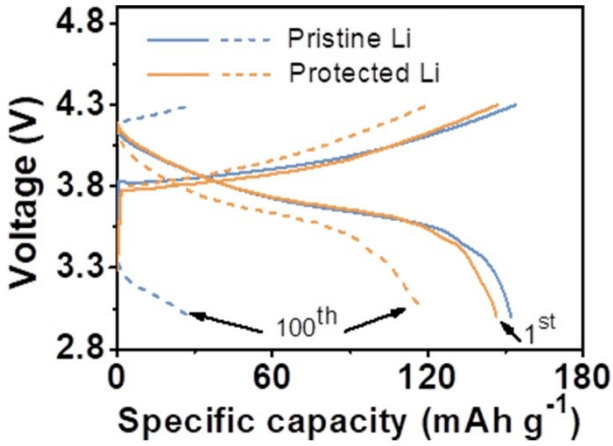

Fig. S11 Voltage profiles of Pristine Li||NCM523 and Protected Li||NCM523 cell.

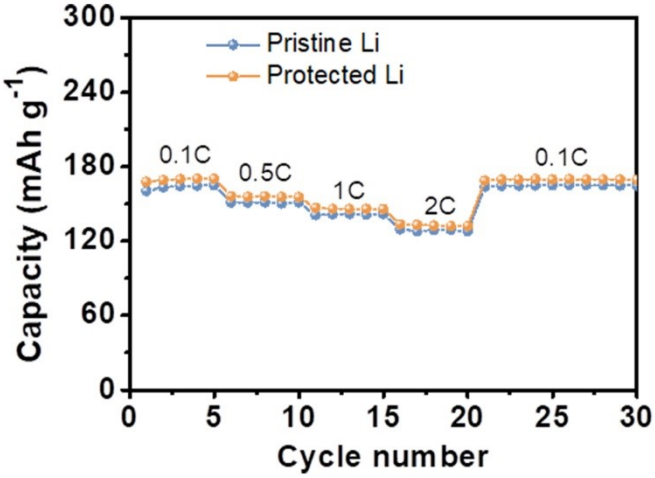

Fig. S12 Rate performance of Pristine Li||NCM523 and Protected Li||NCM523 cell.